Catalytic Growth of Germanium Oxide Nanowires, Nanotubes, and Germanium Nanowires: Temperature-Dependent Effect

Chaoyi Yan, Mei Yin Chan, Tao Zhang, and Pooi See Lee*

School of Materials Science and Engineering, Nanyang Technological University, Singapore 639798, Singapore

Received: September 10, 2008; Revised Manuscript Received: October 28, 2008

One-dimensional GeO_2 and Ge nanostructures, including nanotubes, nanowires, and branched nanowires, were synthesized using Au as catalysts. White products of GeO_2 and brown products of Ge were fabricated at temperature regions of 500−600 and 300−400 °C, respectively. For the first time, we report the formation of single-crystalline GeO_2 nanotubes and branched nanowires. Detailed growth mechanisms of the nanowires, nanotubes, and branched nanowires are presented. Fabrication of one-dimensional nanostructures with different configurations and compositions simultaneously from a single precursor enables the diversity of nanotube/nanowire synthesis, as well as their potential applications in nanoscale photonic and electronic devices.

1. Introduction

Self-assembled one-dimensional (1D) nanostructures are extensively investigated as promising candidates for nanoelectronic, optoelectronic, and photovoltaic applications.[1−3] Semiconductor nanostructures with well-controlled structure, morphology, and chemical compositions are emerging as promising building blocks for nanoscale devices.[4] Various 1D semiconductor nanostructures, including nanowires,[5] nanobelts,[6] and nanotubes,[7] have been successfully synthesized.

Germanium and germanium oxide are of particular interest due to their unique electronic and optical properties.[8,9] The high carrier mobility of germanium and high refractive index to visible light of germanium dioxide are considered for applications in future-electronics and optoelectronic communications. Germanium nanowires have been synthesized through various methods, such as vapor transport,[10] low-temperature chemical vapor deposition,[11] and supercritical solution−liquid−solid method.[12] Several groups also report the successful synthesis of GeO_2 nanostructures, including oxide-enhanced,[13] self-catalytic,[14] and metal-catalyzed growth of GeO_2 nanowires.[15]

Herein, we report the synthesis of GeO_2 and Ge nanostructures from a single precursor with temperature-dependent structures and compositions. GeO_2 nanotubes, branched GeO_2 nanowires, and Ge nanowires were synthesized simultaneously at different growth temperatures. This temperature gradient effect is important to fabricate nanostructures with variable morphologies and compositions resulting in different properties and functionalities simutaneously.[16,17] Growth mechanisms of the 1D nanostructures are presented, promising rationally controlled fabrication of 1D nanostructures with desired configurations, compositions, and hence functionalities.

2. Experimental Section

The nanostructures were synthesized using a high-temperature horizontal quartz tube furnace. In a typical experiment, a small quartz tube containing mixed GeO_2 and carbon powder (molar ratio of 2:3) was loaded into the furnace with mixed powder at the high-temperature end. Si(100) substrates coated with 9 nm Au film were placed at the low-temperature end. The central temperature of the furnace was increased to 1000 °C at a rate of 10 °C min^{-1} and kept for 60 min under a constant Ar flow of 300 sccm (standard cubic centimeter per minute). The substrates are located at temperatures ranging from 300 to 600 °C according to the predetermined furnace temperature profile. The furnace was then switched off and allowed to cool naturally to room temperature. The product color changes from white to brown as the growth temperature decreases from 600 to 300 °C.

Morphology and structure of the products were characterized by X-ray diffraction (XRD, Rigaku) with Cu Kα radiation (λ = 1.5418 Å), field emission scanning electron microscopy (FESEM, JEOL 6340F), and transmission electron microscopy (TEM, JEOL 2010). The chemical compositions were analyzed using energy dispersive spectroscopy (EDS) attached to the TEM. For TEM and EDS analyses, the nanostructures were dispersed in ethanol by ultrasonication for 5 min, and then the solution were dropped on a copper grid coated with holey carbon film.

3. Results and Discussion

3.1. GeO_2 Nanostructures. White products were collected at a synthesis temperature region of 500−600 °C. Figure 1a is a representative low-magnification SEM image of the one-dimensional (1D) nanostructures. Large quantities of nanowires were observed with diameters in the range of 20−200 nm and lengths of tens of micrometers. A high-magnification SEM image of the growth fronts is shown in Figure 1b. Metal catalyst particles can be observed at the nanowire fronts, revealing the VLS growth mechanism.[18] The XRD pattern of the products is shown in Figure 1c. The products are composed of GeO_2 with hexagonal crystal structure (α-quartz-like, JCPDS card 36-1463: a = 4.985 Å, c = 5.648 Å).

Detailed structure and composition analyses of the products were carried out using TEM and EDS. Figure 2a is a typical TEM image of GeO_2 nanowire. The inset is the corresponding selected area electron diffraction (SAED) pattern of the nanowire, recorded along [131] zone axis. Growth direction of the nanowire is [10$\bar{1}$]. EDS spectrum of the nanowire is shown in Figure 2b. The atomic ratio of Ge/O is around 0.5. Peaks of Cu come from the copper grid used for TEM characterization.

* Corresponding author. Phone: (65)-67906661. Fax: (65)-67909081. E-mail: pslee@ntu.edu.sg.

10.1021/jp8080386 CCC: $40.75
Published on Web 01/13/2009

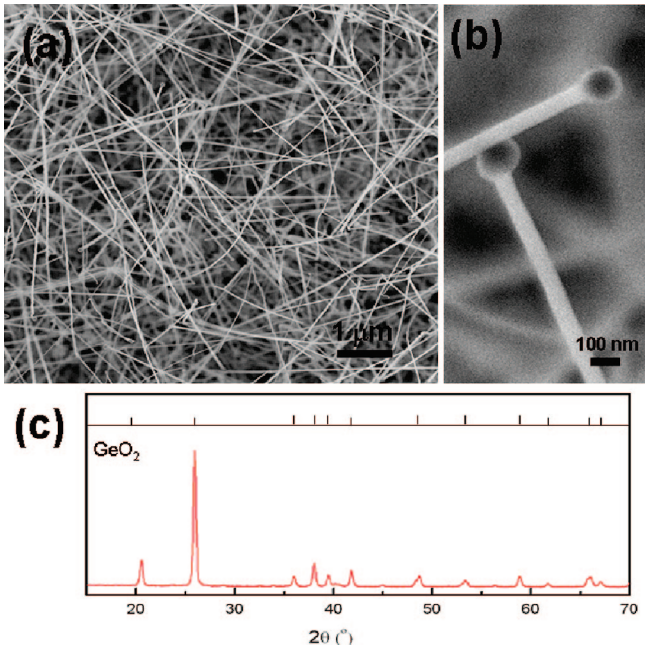

Figure 1. (a) Low-magnification SEM image of the GeO_2 nanowires; (b) high-magnification SEM image showing the catalyst particles at the fronts; and (c) XRD pattern of the products.

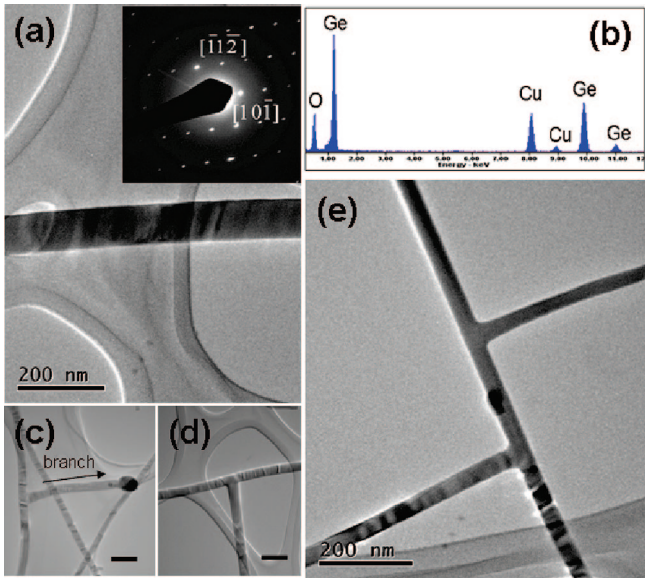

Figure 2. (a) TEM image of GeO_2 nanowire. Inset is the corresponding SAED pattern of the nanowire recorded along [131] zone axis; (b) EDS spectrum of the nanowire; and (c−e) TEM images of branched GeO_2 nanowires. Scale bars in (c,d) are 100 nm.

Around 5% of the nanowires were found to be branched as shown in Figure 2c−e. The short branch (indicated by arrow in Figure 2c) with catalyst particle at the front clearly reveals a process similar to the secondary growth process, where additional catalyst particles are intentionally deposited on the backbone nanowires to direct the growth of branches.[19] The branches show preferential crystal orientation with respect to the axis of the backbone nanowire with the branches growing perpendicular to the backbone. These branched nanowires were widely investigated over many materials.[19,20] The well-defined orientations of the branches with respect to the backbone can be explained by the crystalline structure relation due to epitaxial growth.[19]

GeO_2 nanotubes were also inspected during TEM characterization. Figure 3a is a representative dark field TEM image of a nanotube. The bright field TEM image and corresponding SAED of a nanotube are shown in Figure 3b and c, respectively. The diffraction pattern recorded along [121] zone axis suggests the single-crystalline nature of the nanotube. Although polycrystalline GeO_2 nanotubes have been synthesized through vapor−solid (VS) mechanism,[21] single-crystalline oxide nanotubes are desired for research on the properties and applications considering their better crystallinity.[22] Figure 3d is a TEM image of GeO_2 nanotube with Au catalyst particle at the front. EDS line scanning profiles across a nanotube are shown in Figure 3e. Both Ge and O show depleting signals at the core, verifying the hollow tubular structure.

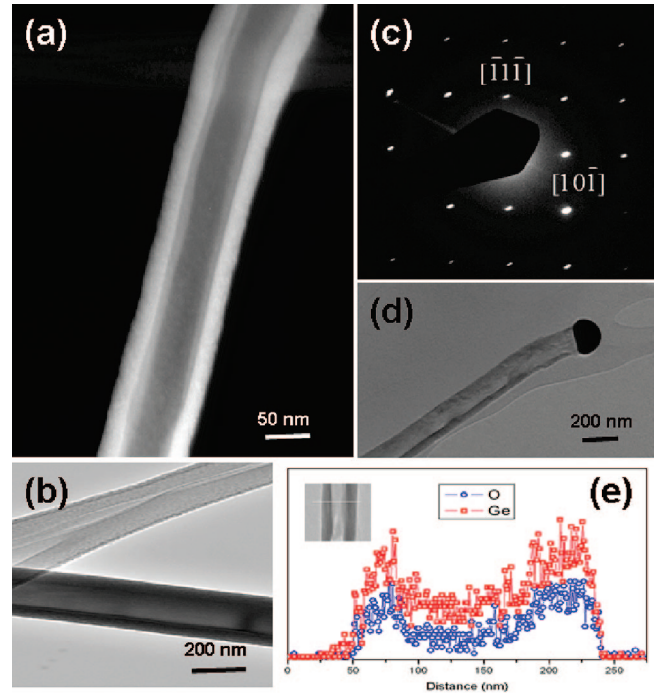

Figure 3. (a,b) Dark field and bright field TEM images of GeO_2 nanotubes; (c) SAED pattern of the nanotube in (b), taken along the zone axis of [121]; (d) TEM image of a nanotube with Au catalyst particle at front, showing the VLS growth mechanism; and (e) EDS line scanning profile across a GeO_2 nanotube.

Unlike other oxide materials, it is worth mentioning that GeO_2 is ultrasensitive to electron beam irradiation.[13,21] The structures of GeO_2 nanowires and nanotubes would change from crystalline to amorphous when exposed to convergent electron beam during HRTEM characterization (Supporting Information, Figure S1).

The product color gradually changes from white to brown between a temperature region of 400 and 500 °C. SEM and XRD analyses of the products in this region reveal a mixture of GeO_2 and Ge nanowires (Supporting Information, Figure S2).

3.2. Ge Nanowires. Brown products grown at 300−400 °C are mainly composed of Ge nanowires. Figure 4a is a typical low-magnification SEM image of the nanowires. The inset of Figure 4a is a TEM image of a Ge nanowire with Au catalyst front. A lattice-resolved HRTEM image of a Ge nanowire taken along [101] zone axis is shown in Figure 4b. The growth direction of the nanowire is ⟨111⟩ as determined from the two-dimensional Fourier transform, which is shown in Figure 4d. The measured lattice spacing of 0.326 nm corresponds to the spacing between (111) planes. EDS spectrum (Figure 4c) reveals that the nanowires are composed of Ge. The small O peak may originate from the thin surface oxide layer of the Ge nanowire (Figure 4b).

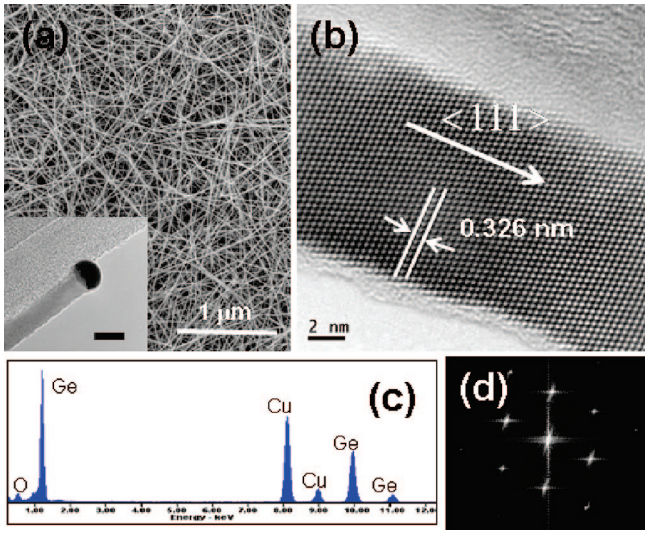

Figure 4. (a) Low-magnification SEM image of Ge nanowires. Inset is TEM image of a single Ge nanowire capped with Au catalyst. Scale bar is 20 nm. (b) HRTEM image and (c) EDS spectrum of a Ge nanowire; and (d) corresponding two-dimensional Fourier transform of the HRTEM image shown in (b).

3.3. Growth Mechanisms Discussion. The temperature-dependent nanostructure configurations and compositions are summarized in Figure 5a. At the central high-temperature region of the furnace, GeO_2 is reduced to Ge through the carbon thermal reduction process,[13,23] as given by:

$$GeO_2 + C \rightarrow Ge + CO_2 \quad (1)$$

Ge with a low melting point would evaporate and be continuously transferred to the low-temperature zone. At a growth temperature of 500−600 °C, GeO_2 nanostructures are formed by precipitation via the oxidation process,[13] as given by:

$$Ge + CO_2 \rightarrow GeO + CO \quad (2)$$

$$GeO + CO_2 \rightarrow GeO_2 + CO \quad (3)$$

Also, it is possible that Ge could react with residual oxygen in the chamber, forming GeO_2. As compared to Ge, oxidation of Si has attracted much more attention due to its dominant role in semiconductor device industry. The thermal-oxidation kinetics of Si were examined in detail over a wide range of oxidation conditions.[24] Particularly, higher temperature was shown to greatly increase the Si oxidation rate.[24] Thus, we also anticipate a similar temperature-dependent oxidation rate for Ge. The oxidation reactions with CO_2 or residual oxygen become significant and dominant only above a certain temperature. Although substoichiometric GeO_x was reported to be oxidized by annealing in air at a temperature as low as 300 °C,[25] the formation of GeO_2 would be remarkably retarded considering the much lower oxidant concentration in the furnace, relative to the abundant oxygen concentration in air. Successive XRD analyses of the products at different growth temperatures from 600 to 300 °C were performed. A decreasing GeO_2/Ge intensity clearly shows the retarded oxidation process at lower growth temperatures (Supporting Information, Figure S3).

The diameter of GeO_2 nanowires is typically larger than that of Ge nanowires, as shown in Figure 2, Figure 4, and schematically depicted in Figure 5a. Although initially coated with Au film of the same thickness, catalyst particles undergo severe coarsening and agglomeration at higher temperature region, which leads to the large diameters of GeO_2 nanostructures. No secondary catalyst particles were intentionally deposited to direct the growth of branched structure in our experiment. Yet for those nanowires at the bottom layer (nearest to the substrate surface), Au nanoparticles may attach to the surface of the backbone nanowire, resulting in branch-growth.[19] A depiction of the branched nanowire growth process is shown in Figure 5b. Also, the Au catalyst particles at high-temperature region have larger particle size due to agglomeration[26] and higher droplet mobility,[27] which increase the possibility of the attachment; hence, branched structures were only inspected at the high growth temperature region.

The growth of single-crystalline GeO_2 nanotubes can be explained by a diffusion limited growth process,[7] as shown in Figure 5c. Both simulation[5] and experimental[7] results indicate that nanotubes can be synthesized via VLS growth mechanism. A diffusion limited growth process leads to higher growth-species concentration at the edges of the catalyst/substrate interface. Consequently, those edges would reach supersaturation first, and the ring-shaped nucleation front leads to nanotube growth.[7] It was observed that the average diameter of GeO_2 nanotubes is larger than that of nanowires. This is because a larger diameter of the catalyst means longer diffusion distance,[5] and this would enhance growth-species concentration in the

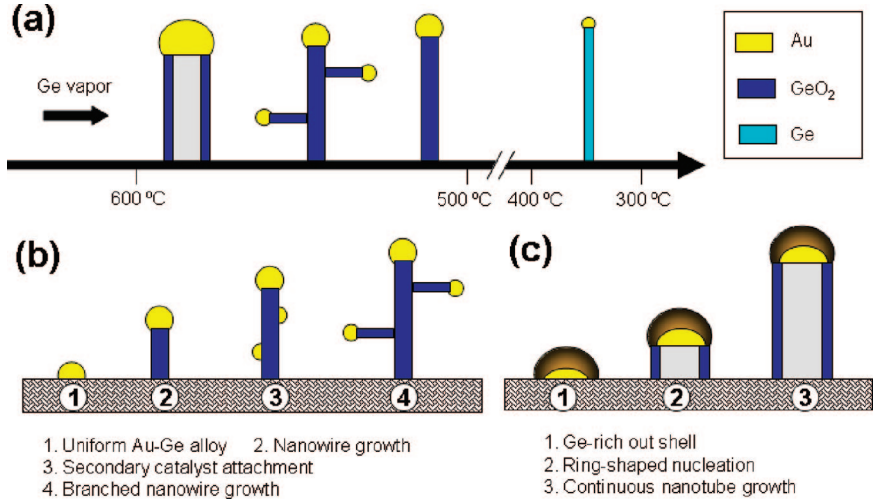

Figure 5. (a) Temperature-dependent nanostructure configurations and compositions; (b) growth process of branched GeO_2 nanowires; and (c) nucleation and growth of GeO_2 nanotubes.

catalyst particle shell, increasing the tendency for nanotube nucleation and growth. Several kinds of nanotubes of different materials synthesized via VLS mechanism have been reported recently.[7,28,29]

According to this scenario, the yield of nanotubes depends on the experimental parameters, such as (i) heating history: A slower heating rate (to 1000 °C) means a longer annealing time. As mentioned above, we expect larger catalyst particles due to agglomeration,[26] which would increase the tendency of nanotube growth. Also, it depends on (ii) Au film thickness: If we initially deposit thicker Au film, the average size of the catalyst particles would also increase. Ideally, there should be a lower bound of the size of Au catalysts, below which the formation of nanotubes would be not observed. This lower bound would change with growth conditions. Thus, with other growth conditions being fixed, we anticipate that a thicker Au film would increase the yield of nanotubes. Finally, it depends on (iii) growth temperature: The ratio of growth rate to diffusion rate is temperature dependent.[7] Qualitatively, the growth rate with respect to diffusion rate would increase at a higher growth temperature, and thus we expect a higher chance of nanotube growth. Although qualitatively, our experiments showed that the growth of nanotubes and nanowires could be explained by the scenario depicted above, quantitative relation is not clear yet and needs further investigations.

4. Conclusion

In summary, GeO_2 one-dimensional nanostructures (nanotubes, nanowires, and branched nanowires) and Ge nanowires were synthesized from a single precursor via VLS growth mechanism using Au as catalyst. At a high growth temperature region of 500−600 °C, white products of GeO_2 were synthesized, while Ge nanowires with a brown color were synthesized at a lower temperature region of 300−400 °C. The single-crystalline nature of all of the nanostructures was confirmed using XRD, TEM, and SAED. The formation of GeO_2 nanotubes was attributed to a diffusion limited growth process. The large Au nanoparticles with mobility higher than those at low-temperature region would attach to the backbone nanowire surface and direct branch growth. The ability to synthesize one-dimensional nanostructures with different configurations and compositions from a single precursor enables the diversity of nanotube/nanowire synthesis. The resultant nanostructures possess substantial opportunities for nanoscale photonic and electronic devices.

Acknowledgment. We thank J. Kasim, Y. Setiawan, P. Darmawan, J. D. Lai, S. S. Pramana, and J. M. Wang for their technical support and insightful discussions. We also thank B. A. Zahara for providing the precursors from the Electron Microscopy & X-ray Diffraction (EMXRD) laboratory.

Supporting Information Available: SEM and SAED of GeO_2 nanowire before and after exposure to convergent electron beam, SEM and XRD of mixed nanowires, and successive XRD spectra. This material is available free of charge via the Internet at http://pubs.acs.org.

References and Notes

(1) Cui, Y.; Lieber, C. M. *Science* **2001**, *291*, 851.
(2) Hu, M. S.; Chen, H. L.; Shen, C. H.; Hong, L. S.; Huang, B. R.; Chen, K. H.; Chen, L. C. *Nat. Mater.* **2006**, *5*, 102.
(3) Tian, B. Z.; Zheng, X. L.; Kempa, T. J.; Fang, Y.; Yu, N. F.; Yu, G. H.; Huang, J. L.; Lieber, C. M. *Nature* **2007**, *449*, 885.
(4) Xia, Y.; Yang, P.; Sun, Y.; Wu, Y.; Mayers, B.; Gates, B.; Yin, Y.; Kim, F.; Yan, H. *Adv. Mater.* **2003**, *15*, 353.
(5) Persson, A. I.; Larsson, M. W.; Stenstrom, S.; Ohlsson, B. J.; Samuelson, L.; Wallenberg, L. R. *Nat. Mater.* **2004**, *3*, 677.
(6) Pan, Z. W.; Dai, Z. R.; Wang, Z. L. *Science* **2001**, *291*, 1947.
(7) Bakkers, E.; Verheijen, M. A. *J. Am. Chem. Soc.* **2003**, *125*, 3440.
(8) Kamata, Y. *Mater. Today* **2008**, *11*, 30.
(9) Xiang, J.; Lu, W.; Hu, Y. J.; Wu, Y.; Yan, H.; Lieber, C. M. *Nature* **2006**, *441*, 489.
(10) Nguyen, P.; Ng, H. T.; Meyyappan, M. *Adv. Mater.* **2005**, *17*, 549.
(11) Wang, D. W.; Dai, H. J. *Angew. Chem., Int. Ed.* **2002**, *41*, 4783.
(12) Hanrath, T.; Korgel, B. A. *J. Am. Chem. Soc.* **2002**, *124*, 1424.
(13) Yuan, C.; Lin, W. T. *Nanotechnology* **2006**, *17*, 4464.
(14) Su, Y.; Liang, X.; Li, S.; Chen, Y.; Zhou, Q.; Yin, S.; Meng, X.; Kong, M. *Mater. Lett.* **2008**, *62*, 1010.
(15) Kim, H. W.; Lee, J. W. *Physica E* **2008**, *40*, 2499.
(16) Pan, A. L.; Yang, H.; Liu, R. B.; Yu, R. C.; Zou, B. S.; Wang, Z. L. *J. Am. Chem. Soc.* **2005**, *127*, 15692.
(17) Liu, Y. K.; Zapien, J. A.; Shan, Y. Y.; Geng, C. Y.; Lee, C. S.; Lee, S. T. *Adv. Mater.* **2005**, *17*, 1372.
(18) Wagner, R. S.; Ellis, W. C. *Appl. Phys. Lett.* **1964**, *4*, 89.
(19) Jung, Y.; Ko, D. K.; Agarwal, R. *Nano Lett.* **2007**, *7*, 264.
(20) Dick, K. A.; Deppert, K.; Larsson, M. W.; Martensson, T.; Seifert, W.; Wallenberg, L. R.; Samuelson, L. *Nat. Mater.* **2004**, *3*, 380.
(21) Jiang, Z.; Xie, T.; Wang, G. Z.; Yuan, X. Y.; Ye, C. H.; Cai, W. P.; Meng, G. W.; Li, G. H.; Zhang, L. D. *Mater. Lett.* **2005**, *59*, 416.
(22) Li, Y. B.; Bando, Y.; Golberg, D. *Adv. Mater.* **2003**, *15*, 581.
(23) Yin, L. W.; Li, M. S.; Bando, Y.; Golberg, D.; Yuan, X. L.; Sekiguchi, T. *Adv. Funct. Mater.* **2007**, *17*, 270.
(24) Deal, B. E.; Grove, A. S. *J. Appl. Phys.* **1965**, *36*, 3770.
(25) Hayashi, S.; Tanimoto, S.; Fujii, M.; Yamamoto, K. *Superlattices Microstruct.* **1990**, *8*, 13.
(26) Hannon, J. B.; Kodambaka, S.; Ross, F. M.; Tromp, R. M. *Nature* **2006**, *440*, 69.
(27) Zhang, D. M.; Guan, L.; Li, Z. H.; Pan, G. J.; Tan, X. Y.; Li, L. *Appl. Surf. Sci.* **2006**, *253*, 874.
(28) Yan, C. Y.; Zhang, T.; Lee, P. S. *Cryst. Growth Des.* **2008**, *8*, 3144.
(29) Yan, Y. G.; Zhou, L. X.; Zhang, J.; Zeng, H. B.; Zhang, Y.; Zhang, L. D. *J. Phys. Chem. C* **2008**, *112*, 10412.

JP8080386